Supporting Information

Froyd et al. 10.1073/pnas.1012561107

SI Text

Aerosol volume measurements for the TC4 campaign are used to calculate the TC4 absolute IEPOX mass concentrations listed in Table 1. These data are publicly available at the NASA ESPO database (http://espoarchive.nasa.gov/archive/arcs/tc4/) and are reproduced here with permission from the investigator, B.E. Anderson. The averages listed below are calculated from total aerosol volume data for cloud-free conditions at latitudes <18N.

$$0\text{–}3 \text{ km: } 5.6 \pm 8.8 \text{ } \mu g\, m^{-3}$$
$$3\text{–}12 \text{ km: } 0.17 \pm 0.49 \text{ } \mu g\, m^{-3}$$

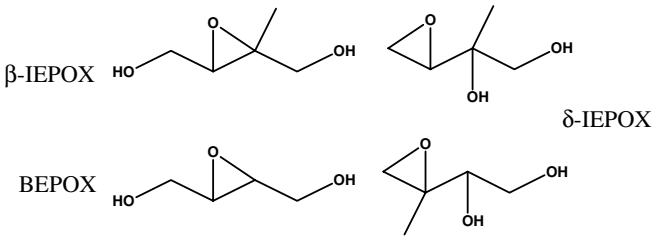

Fig. S1. Structures of isoprene-derived IEPOX and synthesized BEPOX.

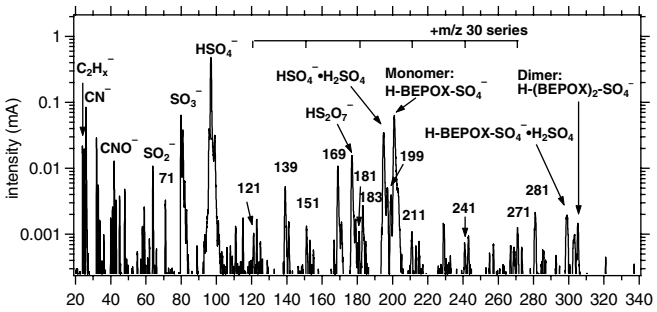

Fig. S2. Single particle mass spectrum of BEPOX uptake products in laboratory-generated acidic sulfate aerosol. The intense peak at m/z 201 is the sulfate ester reaction product. The many smaller peaks above m/z 100 are from other organic species that appear only when BEPOX uptake adds more than approximately 25% mass to the seed aerosol. In particles where BEPOX comprise more than about 25% of the mass, a repeating series of peaks separated by 30 mass units is evident starting at m/z 121. High accuracy mass analysis indicates that this series does not contain sulfate. The 121 ion is probably the tetrol, $HOCH_2(CHOH)_2CH_2O^-$, produced by hydration of BEPOX (1). Adding $-CH_2OH$ units can produce the $+30$ m/z series by forming oligomers of $HOCH_2(CHOH)_nCH_2OH$ or $HOCH_2(CHOH)_m(CH_2O)_nCH_2OH$, similar in structure to the hemiacetal dimer (2). This ion series may also be fragments from larger oligomer chains that were broken down by the PALMS laser ionization. The relatively low signal intensities of the oligomer series is consistent with inefficient ion production from hydroxyl groups and does not necessarily suggest a negligible mass fraction.

1 Surratt JD, et al. (2010) Reactive intermediates revealed in secondary organic aerosol formation from isoprene. *Proc Natl Acad Sci USA* 107:6640–6645.
2 Surratt JD, et al. (2006) Chemical composition of secondary organic aerosol formed from the photooxidation of isoprene. *J Phys Chem A* 110:9665–9690.

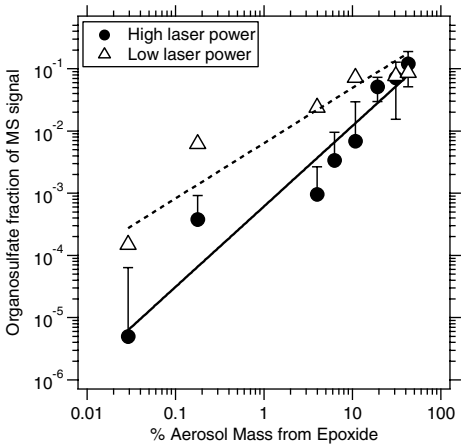

Fig. S3. Mass calibration plot for BEPOX sulfate ester signal in acidic sulfate aerosol. Points are average signal intensities for spectra recorded at high and low ionization laser power (1.8 and 0.4×10^9 W/cm^2). Averages include spectra where the BEPOX signature was below detection limit. Lines are power law fits. Standard deviations are shown for the high power series; low power standard deviations are similar.

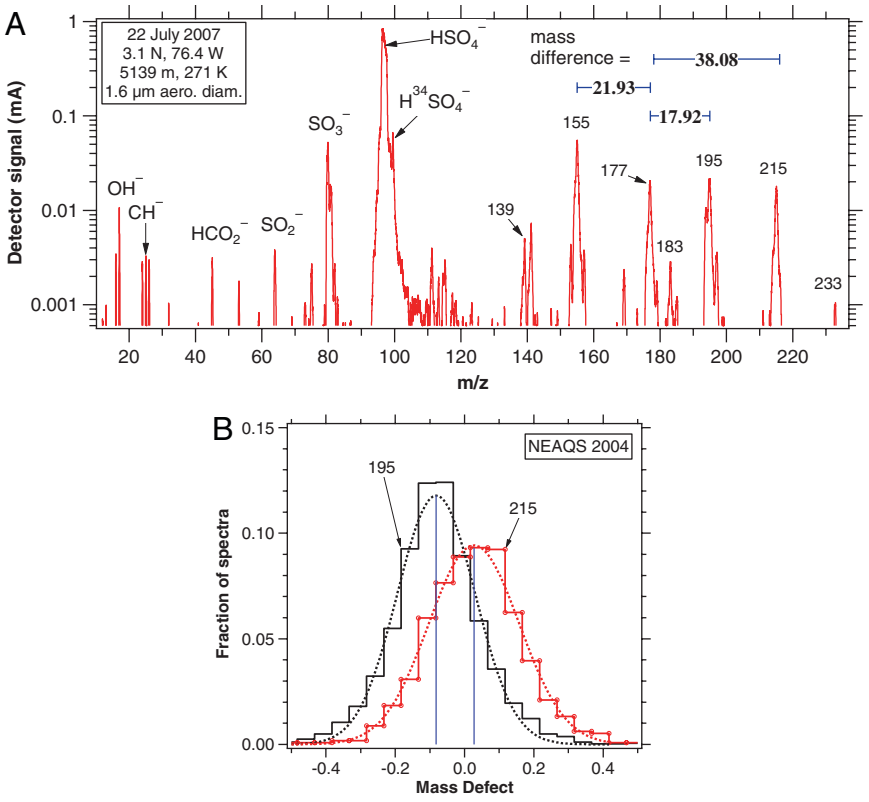

Fig. S4. High accuracy mass analysis of epoxydiol product signatures and other high mass ions. Time-of-flight spectra are recorded at a sampling frequency that can theoretically resolve 0.01 mass units. Although typical mass resolutions are much lower, $\Delta m \sim 0.5$ at m/z 200, the mass difference between two peaks can be determined to an accuracy of 0.01 by averaging many spectra. (*A*) Mass spectrum showing measured mass differences for several peaks relative to the $HS_2O_7^-$ ion at m/z 176.917, which was used as an internal standard. The mass differences for each ion are reported as mass defects (the ion's exact mass—integer mass). (*B*) Histograms of mass defects for two ions determined for all spectra during the NEAQS campaign. Gaussian fits establish the mean mass defect for each ion.

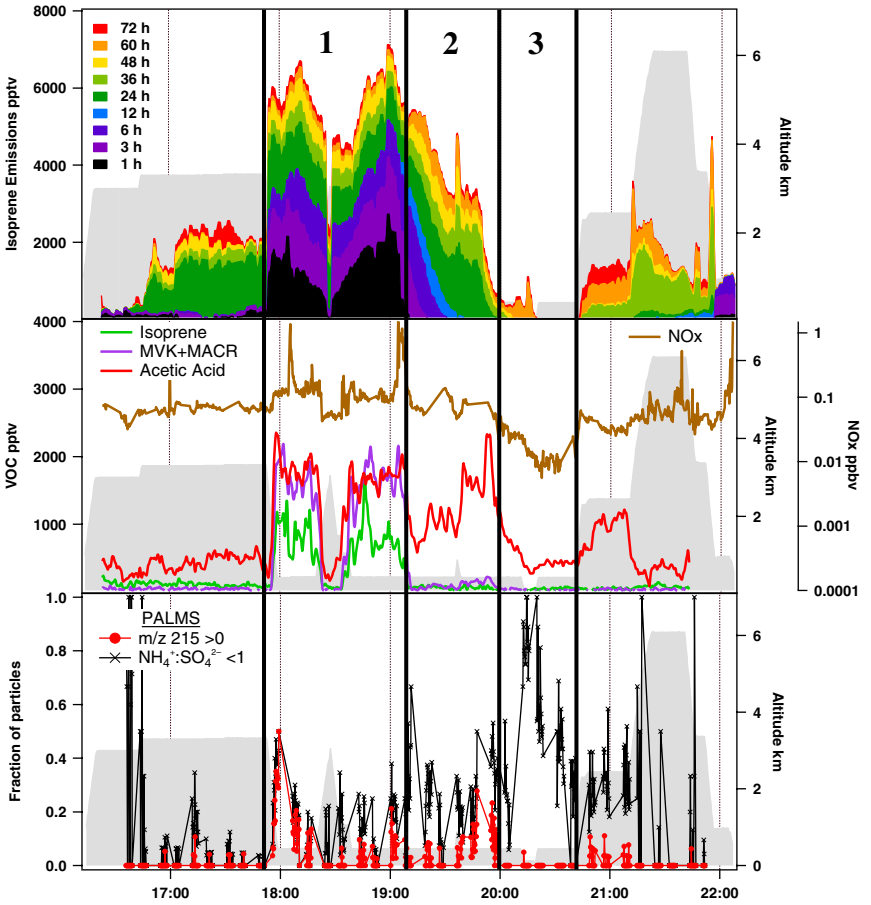

Fig. S5. Time series of the ITCT/NEAQS July 5, 2004, flight over the southeastern United States (see Fig. 3*A*). The top panel shows cumulative isoprene emissions within the previous 72 hours mapped onto the flight track using the FLEXPART trajectory model (1). Gas phase VOCs and NO_x are shown in the middle panel, and fraction of particles with acidic sulfate and isoprene-derived IEPOX sulfate ester signatures (m/z 215) are in the bottom panel. Aircraft altitude is plotted as a shaded gray background. In the top panel, the FLEXPART trajectory model calculates the total isoprene burden (including all oxidation products) along the flight track using isoprene emissions from the Biogenic Emissions Inventory System (BEIS). Measured gas phase VOCs and NOx in the middle panel verify the FLEXPART predictions and demonstrate how the aircraft flew through regions of distinct chemistry during an extended low altitude leg. The bottom panel gives the fraction of aerosol particles that were highly acidic or contained detectable IEPOX sulfate ester. PALMS observed isoprene-derived H-IEPOX-OSO_3^- signatures in acidic aerosols during segment 1, coincident with elevated isoprene and methyl vinyl ketone+methacrolein (MVK+MACR) from emissions within the previous day. Segment 2 further downwind of biogenic emissions also shows IEPOX sulfate ester coincident with elevated acetic acid but little gas phase isoprene, suggesting that the primary biogenic species emitted two days prior, as well as their early stage oxidation products, had been fully oxidized. Acidic sulfate particles were abundant in segment 3, but gas phase VOCs and the trajectory analysis show low isoprene influence, and consequently IEPOX sulfate ester was not observed.

1 de Gouw JA, et al. (2010) Use of the Lagrangian transport model FLEXPART to identify the biogenic contribution to organic carbon species in the gas and aerosol phases. *J Geophys Res-Atmos*, in press.

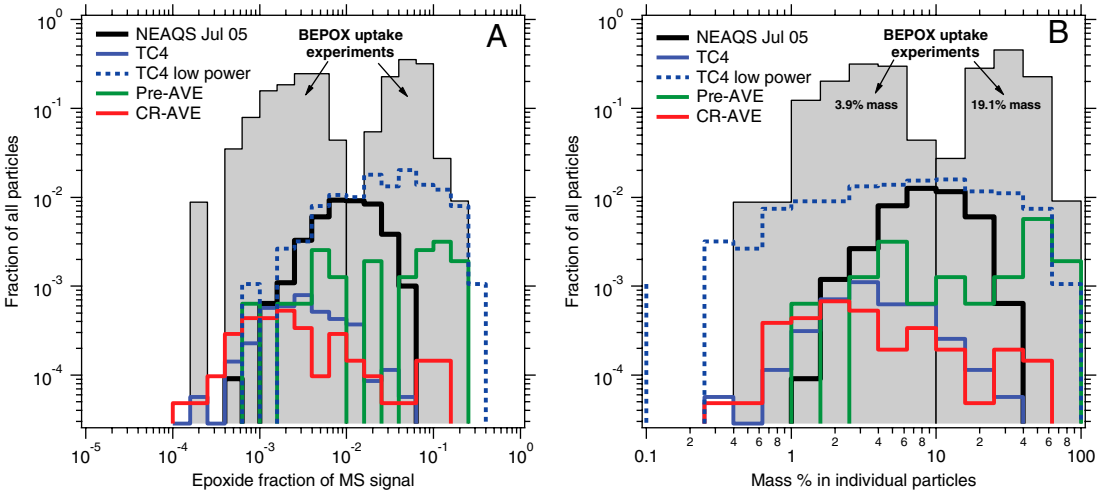

Fig. S6. Abundance of IEPOX sulfate ester observed in individual particles for several aircraft campaigns. (*A*) Histogram of raw signal intensity. The majority of tropospheric particles (92–99%, not shown) did not have a detectable sulfate ester signal using full laser power. However, with reduced laser power IEPOX sulfate ester was detected in about 20 times more particles using during TC4 (dashed line), translating into a larger overall IEPOX mass estimate. (*B*) Percent of individual particle mass attributed to IEPOX calculated using the laboratory calibration. BEPOX abundance for two laboratory calibration experiments is also shown (shaded gray).